From Red Cells to Snowboarding: A New Concept for a Train Track

Qianhong Wu, Yiannis Andreopoulos, and Sheldon Weinbaum*

Departments of Biomedical and Mechanical Engineering & New York Center for Biomedical Engineering, The City College of the City University of New York, 140th Street at Convent Avenue, New York, New York 10031, USA

(Received 16 April 2004; published 3 November 2004)

Feng and Weinbaum [J. Fluid Mech. **422**, 282 (2000)] have shown that there is a remarkable dynamic similarity between a red cell gliding on the endothelial surface glycocalyx and a human snowboarding on fresh powder although they differ in mass by 10^{15}. The lift forces in each case are 4 orders of magnitude greater than classical lubrication theory. Herein we report the first measurements of the pore pressures generated on the time scale of snowboarding and show a feasibility of designing a train that can glide on a track whose permeability and elastic properties are similar to goose down.

DOI: 10.1103/PhysRevLett.93.194501 PACS numbers: 47.55.Mh, 87.10.+e, 87.15.La, 89.40.–a

Biological scientists have wondered, since the motion of red cells was first observed in capillaries, how the highly flexible red cell can move with so little friction in tightly fitting microvessels. In 1996, Vink and Duling [1] conclusively demonstrated *in vivo* that our microvessels are lined with a uniform highly compressible endothelial surface layer (ESL), a glycocalyx of glycoproteins and proteoglycans which varies in thickness from 150 nm in frog mesentery capillaries [2] to 400 nm in hamster cremaster microvessels [1]. At velocities >20 μm/s the red cells appeared to glide above the ESL and there was a narrow intervening fluid gap. However, at velocities <20 μm/s the red cells entered the ESL and when motion was arrested the red cells crushed the glycocalyx and filled nearly the entire lumen of the capillary. In [3], a generalized lubrication theory is developed to describe the pressure and lift forces generated during this motion. This theory, which applies to one- or two-dimensional planar lifting surfaces, shows that the principal difference between a red cell squeezing through a tightly fitting capillary and a human snowboarding is the substantial loss of pore pressure that occurs due to leakage at the lateral edges of the snowboard. The analysis in [3] shows that the behavior is governed by three dimensionless groups, a dimensionless permeability parameter, $\alpha = h/K^{1/2}$, where h is the thickness of the porous layer and K is its Darcy permeability, the slope λ of the planing surface, and its length to width ratio L/W. For $\alpha \gg 1$, the lift forces increase as α^2 for all λ. The dramatic increase in lift for large α is due to the fact that the fluid is transiently trapped within the soft porous material and cannot escape on the time scale of the motion.

It is well known that sliding friction in skiing on snow is greatly reduced by the presence of μm thick fluid films that form beneath the ski due to frictional heating [4]. This film greatly reduces friction drag in cross-country skiing much like the thin fluid film that exists between the red cell membrane and the edge of the ESL when the red cell is moving at velocities >20 μm/s. At velocities <20 μm/s, the basic mechanism by which the red cell is able to reduce its drag once it enters the glycocalyx is described in [5], where it is shown that the normal force required to compress the core proteins in the glycocalyx is 2 orders of magnitude smaller than the lift force due to the fluid draining pressure. Since sliding friction over the solid phase is proportional to this force, frictional drag is greatly reduced.

Whereas it would be very difficult to measure the excess pore pressure that develops during red cell motion, an equivalent experiment can be easily performed for snow. To our knowledge, no one has ever attempted to measure the draining pressure that builds up in snow on a time scale characteristic of skiing or snowboarding. There is extensive literature on the behavior of snow during uniaxial compression [6,7], but these studies examine the compression of snow and its creeping behavior on time scales much longer than that of interest herein. In Fig. 1, we show a novel piston cylinder apparatus with Rigimesh sidewalls that will filter snow crystals whose size is greater than 0.120 mm. The mesh is a sintered arrangement of screens with negligible airflow resistance. The piston and a probe mounted on the bottom plate are instrumented with high-frequency, subminiature pressure transducers fabricated by Kulite Semiconductor Products, Inc. These transducers are able to measure

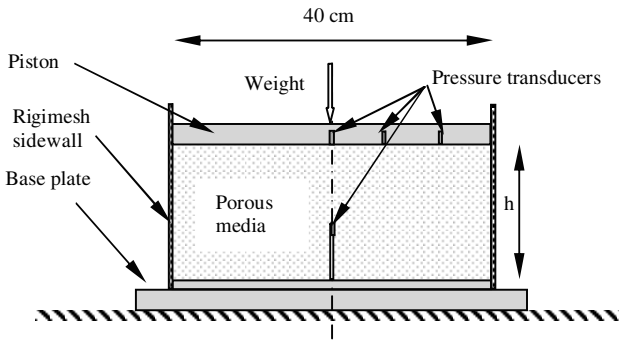

FIG. 1. Schematic of dynamic snow compression apparatus.

millisecond variations in dynamic pore pressure on the underside of the piston and on the center line of the cylinder when a weighted piston is dropped from rest. The diameter of the piston, $D_{\text{piston}} = 40$ cm, is chosen to be representative of the dynamic response that one would encounter while snowboarding. The electrical output is collected with an Iotech 488/8 data acquisition system and finally transferred to a computer for further processing.

A balance of forces acting on the piston in Fig. 1 requires that

$$m\frac{d^2h}{dt^2} = -mg + F_{\text{air}} + F_{\text{solid}}, \tag{1}$$

where m is the mass of the piston, h is its instantaneous height, F_{solid} is the force exerted by the solid phase, and F_{air} is the integral of the pore air pressure $P(r, h, t)$ at the piston surface,

$$F_{\text{air}}(t) = \int_0^R 2\pi r P(r, h, t)dr. \tag{2}$$

The instantaneous flow in the device is approximately described by a quasisteady axisymmetric flow that satisfies Darcy's law (3a) and the continuity Eq. (3b) [8]:

$$\mathbf{q} = -\frac{K}{\mu}\nabla P, \tag{3a}$$

$$\nabla \cdot (\rho \mathbf{q}) + \frac{\partial(\rho\varphi)}{\partial t} = 0, \tag{3b}$$

where μ and ρ are the viscosity and density of the air, respectively, $\mathbf{q}$ is the specific flux vector, and ϕ is the porosity. For axisymmetry and $\rho = \text{const}$ Eqs. (3a) and (3b) can be combined to yield a Poisson equation:

$$\frac{1}{r}\frac{\partial}{\partial r}\left(r\frac{\partial P}{\partial r}\right) + \frac{\partial^2 P}{\partial z^2} + \frac{\mu}{K}\frac{h_0(\phi_0 - 1)}{h^2}\frac{dh}{dt} = 0, \tag{4}$$

where h_0 and ϕ_0 are the initial thickness and initial porosity of the porous layer, respectively. K is a function of compression and is given by Shimizu's empirical relationship [9], $K = 0.077\exp(-0.0078\rho_s)d^2$, where d is the mean diameter of the snow particle and ρ_s is the snow density. The solution of Eq. (4) satisfying the boundary conditions, $q_z|_{z=0} = 0$, $q_z|_{z=h} = dh/dt$, $\partial P/\partial r|_{r=0} = 0$, $P|_{r=R} = 0$, is given by

$$P(r, z, t) = \left[\sum_{k=1}^{\infty} \frac{-\frac{\mu}{K}\int_0^R rJ_0(\lambda_k r)dr}{\sinh(\lambda_k h)\lambda_k \int_0^R rJ_0^2(\lambda_k r)dr} J_0(\lambda_k r) \times \cosh\lambda_k z + \frac{\mu(R^2 - r^2)}{4K}\frac{h_0(\phi_0 - 1)}{h^2}\right]\frac{dh}{dt}, \tag{5}$$

where λ_k are roots of $J_0(\lambda_k R) = 0$. Substituting Eq. (5) into (2), one can readily obtain $F_{\text{air}}(t)$.

In (1), F_{solid} is determined by an independent quasistatic experiment, in which one starts with a lightweight piston, which is typically 1/10 the weight of the heavy piston used in the dynamic experiment, and incremental weights of comparable magnitude are added till one achieves the weight of the piston used in the dynamic experiment. In this experiment, the air in the pores can slowly escape without elevating the pore pressure, in contrast to the dynamic experiments in which the air is temporarily trapped before it escapes. After each incremental weight is added, the compression Δh of the snow layer is measured. This provides an empirical expression for F_{solid}:

$$\frac{F_{\text{solid}}}{F_{\max}} = f\left(\frac{\Delta h}{\Delta h_{\max}}\right), \tag{6}$$

where $F_{\max} = mg$ and $\Delta h_{\max}$ is the final displacement of the piston when the full load mg is applied. Equation (6) is nonlinear for both snow and a material with the properties of goose down, which are considered shortly. When $\Delta h/\Delta h_{\max} < 0.3$, the force exerted by the solid phase is small, whereas when $\Delta h/\Delta h_{\max}$ approaches unity the excess pore pressure has been drained and the solid phase supports the entire load.

Using (2), (5), and (6), one can integrate Eq. (1) subject to initial conditions, $h|_{t=0} = h_0$, $dh/dt|_{t=0} = 0$, numerically. The solution for $h(t)$ is then substituted into (5) to determine the pore pressure distribution.

In Fig. 2(a) we have plotted the results for the time-dependent variation of the pore pressure at the location of the central pressure transducer on the underside of the piston after it is released from rest. Natural wind-packed soft snow, with an ambient temperature of $-10\,^{\circ}\text{C}$, was used in this experiment. One observes a rapid rise in pore pressure and then a decay that occurs on a time scale of roughly 0.8 s. The characteristic time to drain the air can be gleaned from a simple drainage model, $t_c = \mu\pi R^2/(8P_c K)$, where $P_c = mg/\pi R^2$. In the current application, one finds that $t_c \approx 1$ s for $K = 5.0 \times 10^{-10}$ m^2 and $m = 5.9$ kg. Since the length of time that a 1.5 m snowboard would be in contact with a given patch of snow if it were traveling at 10 m/s would be 0.15 s, it is clear from the figure that after 0.15 s the excess pore pressure has only started to relax and much of the weight of the snowboarder would be supported by the air that is still trapped in the partially compressed snow layer. The solid curves in Fig. 2(a) are our theoretical model predictions for the time-dependent decay of the excess pore pressure. One notes that there is one value of the initial Darcy permeability K_0, 5.0×10^{-10} m^2, which provides a best fit to the experimental data.

The behavior just described suggests that it might be possible to support very heavy loads on very soft porous materials, provided the time of passage of the planing surface is small compared to the time that it would take

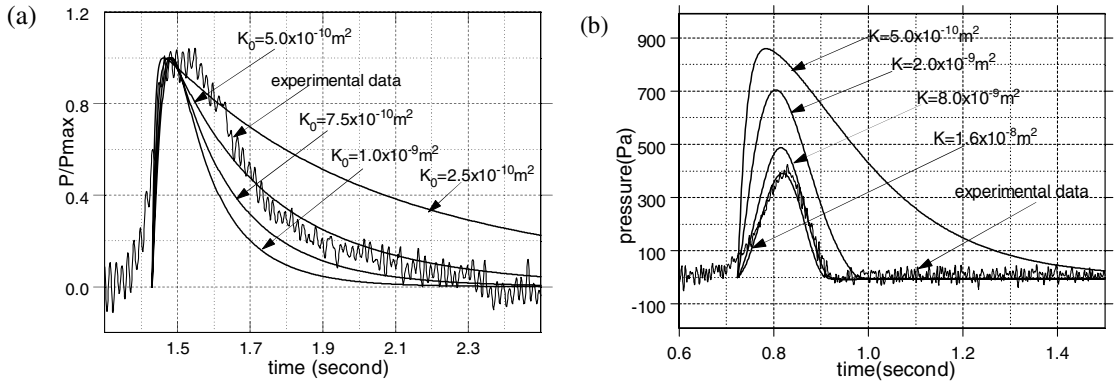

FIG. 2. Time-dependent pressure at the center of the piston and its comparison with the predictions of Eq. (5) during dynamic compression experiments in the porous cylinder-piston apparatus. (a) For snow, $m = 5.9$ kg, $h_0 = 11.43$ cm, $\Delta h_{\max}/h_0 = 0.22$, and $P_{\max} = 788$ Pa. (b) For goose down, $m = 6.4$ kg, $h_0 = 12.77$ cm, $\Delta h_{\max}/h_0 = 0.35$, and $P_{\max} = 400$ Pa.

for the confined air or fluid to drain from the porous media beneath it. The calculations in [3] show that the air trapped in snow can easily support the weight of a 70 kg snowboarder when $K_0 < 10^{-8}$ m^2. For a snowboard whose surface area is 0.5 m^2, the pore pressure required is approximately 1/75 of an atmosphere or 1.4 kPa. The slope λ of the snowboard will depend on its velocity U. The feasibility of supporting a 50 ton high-speed train car whose planform is 25 m long ($L = 25$ m) and 2 m wide ($W = 2$ m) can be gleaned from the fact that the average excess pore pressure required will be 9.8 kPa, or only 7 times that of the snowboard. This is easily realizable for a porous material whose permeability is of order 10^{-8} m^2 or smaller, provided the loss of pressure through lateral leakage is eliminated. Furthermore, if the deformation of the solid phase is small, that is $\Delta h/\Delta h_{\max} \ll 1$, the load bearing force of the solid phase will be small, and sliding friction greatly reduced. We now show that a synthetic material with the mechanical properties of goose down is ideal for these purposes. This material has the additional important advantage that after compression it has a weak restorative force in contrast to snow, which has no elastic recoil.

To measure the dynamic compression properties of goose down, we have used the same porous cylinder apparatus shown in Fig. 1. These results, which are analogous to those just described for wind-packed snow, are shown in Fig. 2(b). One observes again that there is one value of K, 1.6×10^{-8} m^2, which provides a best fit of the experimental data. The principal difference between the curves in Figs. 2(a) and 2(b) is that there is no extended relaxation phase for the goose down since the dimensions of the piston are too small and the value of K too large for the excess pore pressure to support most of the piston weight. The maximum pore pressure is only 400 Pa, about half of that needed. However, if $t_c = \mu\pi R^2/(8P_cK)$, the diameter of the piston were 25 m (the length of a train car), and the time to travel this distance 3 s (velocity only 8.3 m/s), the maximum pore pressure would increase to 50 kPa. These scaling arguments predict that a planform of 25 m length and 2 m width would have a maximum possible lift of approximately 250 metric tons for K of order 10^{-8} m^2.

In Fig. 3, we show a schematic of our proposed lift enhanced, goose down filled train track. The top surface on which the planform glides is a highly flexible porous sheet through which the pore pressure in the porous medium is transmitted. To prevent lateral leakage of pressure the sidewalls of the track are made of an impermeable membrane that is supported by rigid sidewalls. The only significant leakage of pressure occurs at the front and back ends of the planform where the pressure is that of the ambient air. At low speeds, when the velocity of the train car is not sufficient for its weight to be supported by the trapped air in its long slender rectangular shaped goose down pillow, one resorts to wheels. Once the speed has increased to a value sufficient to support the car, the wheels are raised.

The performance of our enhanced lift 50 ton train car is plotted in Fig. 4, where the track height h_2 at the leading edge is 10 cm. These theoretical predictions are based on the solution of the generalized Reynolds equation (2.25) in [3], which, in the large α limit, reduces to

$$\frac{d}{dx}\left(-\frac{1}{\alpha^2}\frac{dp}{dx}h\right) = \frac{dh}{dx}, \tag{7}$$

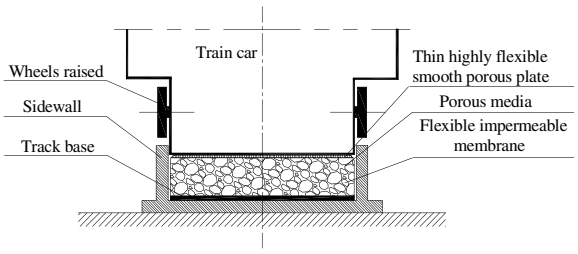

FIG. 3. Sketch of the new train model in the transverse plane (not to scale).

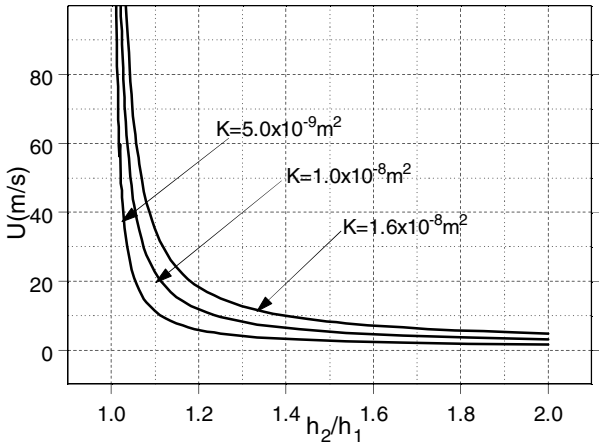

FIG. 4. The velocity U required to support a train car of 50 metric tons gliding on a porous track as a function of h_2/h_1 for various K. Note that for $U > 35$ m/s, $h_2/h_1 < 1.1$. $L = 25$ m, $W = 2$ m, and $h_2 = 0.10$ m.

where $p = P/(\mu LU/h_2^2)$. For each U, the ratio $k = h_2/h_1$ of the leading to trailing edge heights is determined so as to support the train car weight. K in our experiments in Fig. 2(b) is based on goose down from inexpensive pillows with larger, more porous feathers. One observes that even for this coarser goose down, where $K = 1.6 \times 10^{-8}$ m^2, h_2/h_1 will be <1.4 and the slope $\lambda = \tan\beta < 0.001$ if the car velocity is >10 m/s. Moreover, the performance curves are highly nonlinear and at high speeds in excess of 35 m/s there is less than a 10% compaction of the track at the trailing edge. For such small compactions our static compression experiments show that the lift force generated by the solid phase will be $<2\%$ of the lift force due to the pore pressure.

The force diagram in Fig. 5 provides an overview of the global force balance on the moving train car. In this figure U is the velocity of the train car; N_a and N_s are the normal forces due to air and goose down, respectively; T is the force due to solid sliding friction, $T = \eta N_s$, where η is the sliding friction coefficient; D is the aerodynamic drag, $D = C_D A\rho U^2/2$; and the mass of the train is m. Using this model we estimate that for $U = 50$ m/s and $\eta = 0.15$, the force due to sliding friction will be about $1/5$ of the aerodynamic drag on a streamlined train car and the pore pressure lift force more than 300 times greater than the sliding friction force and 50 times the total drag. The total drag includes T, D, and the planform drag $(N_a + N_s)\sin\beta$ due to the very small tilt angle β of the planing surface. $N_s \sin\beta$ is negligible and $N_a \sin\beta$ is only 8% of T. Sliding friction can never approach rolling friction where the friction coefficient is only 0.001. However, our objective is simply to reduce sliding friction to a level where it is small compared to other drag forces. With proper design, the new train car should be able to negotiate turns with remarkable ease and little sidewall friction. Both sides of the car planform could be arched inwards (concave) to turn in either direction on a curved track of adequate turning radius, unless the planform is able to deform in its own plane. Sidewall friction can be nearly entirely eliminated by having retractable horizontal wheels in the sidewalls near the front and back edges of the planform. These wheels will resist the appreciable centripetal forces that will occur during high-speed turns, and the track must be banked accordingly.

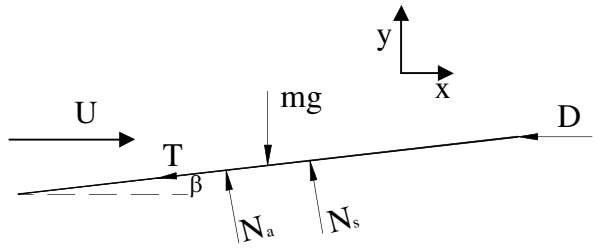

FIG. 5. Forces on the train car. Here U is its velocity, N_a and N_s are the normal forces due to air and goose down, respectively, T is the force due to solid sliding friction, and D is the aerodynamic drag.

The use of soft porous materials to produce planar lifting surfaces with dramatically enhanced lift and greatly reduced drag is a new concept in lubrication theory. The application to snowboarding and the design of a futuristic train track were chosen for their novelty, but the basic concepts could have an important application in the design of soft porous bearings with greatly increased lubrication pressures and long life. Whereas goose down is an expensive, impractical material, there are many synthetic fiber fill materials with comparable mechanical properties.

Parts of this research relating to the endothelial glycocalyx were supported by NHLBI Grant No. HL-44485.

*Corresponding author.
Electronic address: weinbaum@ccny.cuny.edu

[1] H. Vink and B. R. Duling, Circ. Res. **79**, 581 (1996).
[2] J. M. Squire *et al.*, J. Struct. Biol. **136**, 239 (2001).
[3] J. Feng and S. Weinbaum, J. Fluid Mech. **422**, 282 (2000).
[4] S. C. Colbeck, J. Sports Sci. **12**, 285 (1994).
[5] S. Weinbaum *et al.*, Proc. Natl. Acad. Sci. U.S.A. **100**, 7988 (2003).
[6] M. Mellor, J. Glaciol. **19**, 15 (1977).
[7] L. H. Shapiro, J. B. Johnson, M. Sturm, and G. L. Blaisdell, USA Cold Regions Research and Engineering Laboratory Research Report No. 97-3, 1997.
[8] J. Bear, *Dynamics of Fluids in Porous Media* (Elsevier, New York, 1972).
[9] H. Shimizu, Institute of Low Temperature Science, Sappora, Japan, Contribution No. 1053, 1970 (in English).